Extruded versus solvent cast blends of poly(vinyl alcohol-*co*-ethylene) and biopolymers isolated from municipal biowaste

Flavia Franzoso,[1] Carlos Vaca-Garcia,[2,3] Antoine Rouilly,[2,3] Philippe Evon,[2,3] Enzo Montoneri,[4] Paola Persico,[5] Raniero Mendichi,[5] Roberto Nisticò,[1] Matteo Francavilla[6]

[1]Università Di Torino, Dipartimento Di Chimica, via P. Giuria 7, Torino, 10125, Italy
[2]Université De Toulouse, INP, Laboratoire De Chimie Agro-Industrielle, ENSIACET, 4 Allée Emile Monso, BP 44362, 31030 Toulouse Cedex 4, France
[3]INRA, Laboratoire De Chimie Agro-Industrielle, Toulouse Cedex 4, 31030, France
[4]Biowaste Processing, via XXIV Maggio 25, Verona, 37126, Italy
[5]Istituto per Lo Studio Delle Macromolecole (ISMAC-CNR), via E. Bassini 15, Milano, 20133, Italy
[6]STAR Integrated Research Unit, Università Di Foggia, via Gramsci, 89-91, Foggia, 71121, Italy
Correspondence to: E. Montoneri (E-mail: enzo.montoneri@gmail.com)

ABSTRACT: Water-soluble biopolymers (SBO) were isolated from the alkaline hydrolysate of two materials sampled from an urban waste treatment plant; that is, an anaerobic fermentation digestate and a compost. The digestate biopolymers contained more lipophilic and aliphatic C, and less acidic functional groups than the compost biopolymers. The SBO were blended with poly (vinyl alcohol-*co*-ethylene), hereinafter EVOH. The blends were extruded and characterized by FTIR spectroscopy, size exclusion chromatography (SEC)– multi angle static light scattering (MALS) analysis, and for their thermal, rheological, and mechanical properties. The blends behavior depended on the type of SBO and its relative content. Evidence was obtained for a condensation reaction occurring between the EVOH and SBO. The best results were obtained with the blends containing up to 10% SBO isolated from the biowaste anaerobic digestate. Compared with the neat EVOH, these blends exhibited lower melt viscosity and no significant or great difference in mechanical properties. The results on the extrudates, compared with those previously obtained on the same blends obtained by solvent casting, indicate that the blends properties depend strongly also on the processing technology. © 2015 Wiley Periodicals, Inc. J. Appl. Polym. Sci. **2016**, *133*, 43009.

INTRODUCTION

The manufacture of blends of synthetic polymers and new bio-based polymers is a current research trend to reduce the exploitation of chemicals from fossil sources and consequently lower carbon dioxide emission.[1,2] Whereas much research has been devoted to natural biopolymers from dedicated crop, little work has been carried out on biopolymers obtained from biowastes. Very recently, blends of soluble biopolymers (SBO) isolated from municipal biowastes and agriculture residues with poly vinyl alcohol-*co*-ethylene (EVOH) and poly ethylene-*co*-acrylic acid (PEAA) have been reported.[3–5] The SBO were constituted by a pool of macromolecules with weight-average molar masses (MWs) of 67 to 463 kDa, which contain aliphatic and aromatic C chains bonded to carboxylic, phenol, and amino groups. They were blended with EVOH to obtain films by solvent casting. This technology, however, required the use of organic solvents obtained from fossil source. As the SBO blends prepared

in this fashion exhibited interesting mechanical properties, compared with the neat synthetic polymers, it seemed worthwhile to carry on further process and product development work. The present article reports the preparation by extrusion and characterization of the EVOH–SBO blends and the comparison of their properties with the EVOH–SBO blends previously obtained by solvent casting. Compared with solvent casting, extrusion is a more industrially relevant technique, used in particular for film packaging applications (extruded sheets, blown films, etc.). Being carried out in the absence of solvents,[6] it was investigated as potentially greener process alternative. In addition, extrusion occurs with the reagents in the melt state, resulting not only in large differences in temperature but also in residence time and applied shear rate compared with the solvent cast technique. Thus, the extruded blends were expected to be new materials. In this fashion, the *vis-a-vis* comparison of extrusion and solvent casting, performed with the same reagents
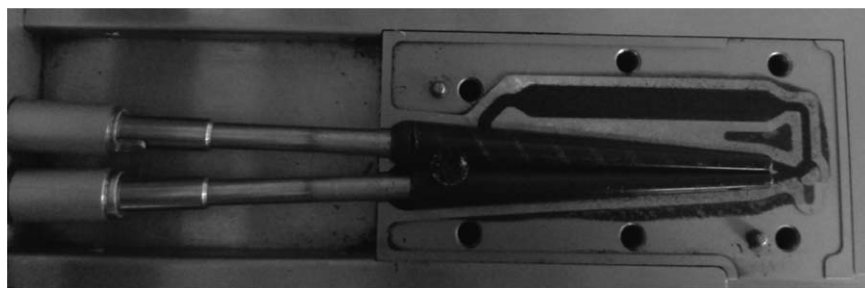
Figure 1. MiniLab microcompounder with the black sample in the recirculation chamber.

could be accomplished. Products' expectations were based on the following facts.

For the EVOH–SBO blends prepared by solvent casting,[3,4] a condensation reaction between the EVOH hydroxyl groups and the SBO PhOH functional groups was found to occur at 120°C. This led to the formation of a new material containing SBO covalently bonded to EVOH. The product was a mix of a crystalline phase containing 3 to 5% SBO and of an amorphous phase containing 34 to 49% SBO. Upon increasing the SBO and/or the amorphous phase content in the blend, the product, compared with neat EVOH, presented the following features: up 3× higher weight average molecular weight (M_w), lower melting enthalpy (ΔH_m), higher glass transition temperature (T_g), no change in melting temperature (T_m), and lower cold crystallization temperature (T_c). In addition, the films containing 5.9% SBO and characterized by the highest molar mass exhibited the highest Young modulus (1082 MPa) and a decrease in the strain at break to 42.3%. At higher SBO amounts, the Young modulus and strain at break values were lower than those of the neat EVOH were. These results prospected that new materials with modified thermal and mechanical properties could be developed by reacting a synthetic polymer containing hydroxyl groups and the waste sourced SBO biopolymers. It was therefore interesting to assess if the EVOH–SBO blends were obtained also by extrusion, and how chemical structure and properties of the extruded products compared with those of the products obtained by solvent casting. Indeed, different processes produce materials with different properties, which may affect the end use. Extrusion is still the industry workhorse.[7] Extrusion requires mixing and homogenizing the ingredients in the melt state. In the case of EVOH melting at 176°C, and SBO not melting and decomposing above 220°C, extrusion had to be carried out in this temperature range. Under these circumstances, it was deemed likely that the interaction between the EVOH and SBO in this temperature range during extrusion was different compared with that occurring at 120°C during solvent casting, and that this affected significantly the nature of the blend product. The perspective to provide SBO-EVOH blends with a range of different properties, starting from the same reagents by using different manufacturing processes, offered worthwhile scope for the present work.

EXPERIMENTAL

Materials

The SBOs, hereinafter named with the acronym FORSUD and CV, were sourced from municipal biowastes sampled from two different streams of the ACEA Pinerolese waste treatment plant in Pinerolo, Italy. These were the digestate (FORSUD) recovered from the plant biogas production reactor fed with the organic humid fraction from a separate source collection of urban refuse and the compost (CVT230) obtained from home gardening and park trimming residues aged for 230 days under aerobic conditions. The two SBOs were isolated as black powders from the alkaline hydrolysates of the digestate and compost, and were characterized as previously reported.[8] Pellets of EVOH, poly (vinyl alcohol-*co*-ethylene) with 38 mol % ethylene, commercial name Soarnol (CAS number 26221-27-2) were supplied by Nippon Gohsei Europe GmbH (Dusseldorf).

Samples Preparation and Rheological Measurements

The SBO and EVOH were previously ground and left in an oven set at 50°C overnight to eliminate eventual water adsorbed on the surface. Then, each type of SBO was hand-blended with EVOH at different ratios and introduced in a MiniLab microcompounder by Thermo Scientific Haake, Germany (Figure 1). This equipment consists in a co-rotating twin-screw configuration. It is equipped with a backflow channel designed as a slit capillary. Pressure is measured at the capillary entrance and exit, and shear stress is deduced from the pressure drop during melt polymer recirculation. The change in screw speed leads to different relative shear rates. In this work, measurements with this equipment were made at 200°C with screw speeds from 50 to 200 rpm corresponding to relative shear rates between 177 and 711 s^{-1}. All samples were prepared with the same procedure. The chamber was heated up to 200°C and kept at this temperature during the measurements. When the chamber was at 200°C and the screw speed set at 50 rpm, the EVOH–SBO mix was added in three aliquots helped by a piston. The sample was recirculated in the MiniLab microcompounder for 8 min. During this time, the screw speed was increased from 50 to 200 rpm. This was achieved in seven steps, that is, 50-75-100-125-150-175-200 rpm. Afterward, the screw and the measurement were stopped, and the chamber was cooled with compress air. For each sample, the chamber was open when the internal sensor registered a temperature of 120°C. As reported elsewhere,[9] measured viscosities and shear rates are called "relative," as volumetric flow through the backflow channel is not set but just estimated thanks to the screw speed. Indeed, it is correlated proportional to the screw speed, and the universal $8e^{-7}$ proportionality coefficient used here corresponds to that of polyolefins. Slip effects along the device wall could also cause deviation from absolute viscosity values, as stated on the device's technical
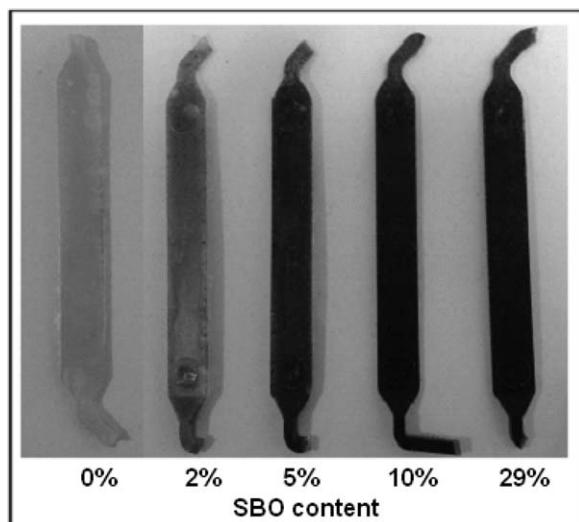
Figure 2. Samples collected from MiniLab compounder prepared with EVOH and different content of FORSUD.

documentation. Viscosities in this study are so only relative, that is, apparent. It has been noted that a recent work using also the MiniLab microcompounder developed a new methodology based on the Hagen–Poiseuille theory to determine real viscosities of non-Newtonian fluids like PP/PA6 polymeric blends.[10] The latter was not used in the present work. However, the comparison of relative viscosities of various EVOH/SBO blends remained possible, especially as the polymeric matrix used was the same in all blends. For further characterization, extruded samples were collected from the backflow channel. These samples were in rod form about 90-mm long, 10-mm large, and 1.5-mm thick. They were stored at 25°C and 60% of relative humidity prior to testing. As typical examples of extrudates, Figure 2 shows the samples obtained from neat EVOH and from the EVOH blends containing 2 to 29% FORSUD. The sample color intensity is contributed by the SBO. The SBOs were obtained by alkaline hydrolysis of the sourcing materials, followed by filtration through 5 kD polysulfone membranes and drying of the membrane retentate.[8] Because of their complex heterogeneous chemical composition (see "Results and Discussion" section), no attempts were made to purify and/or bleach the SBOs before blend melting.

Selective Extraction Experiments

The blend sample was suspended in aqueous $1M$ NaOH at 1/100 w/V ratio and kept 4 h at room temperature or heated 4 h at 60°C. The blend sample was then withdrawn from the water phase, washed with water to pH 6, dried, and weighed. The starting and recovered blend samples were analyzed for their N content. The N content was taken as indicator of the blend SBO content, based on the amount of the neat SBO reported in Table I. The amount of SBO released from the starting blend samples following the alkali treatment was calculated based on both its total weight and N loss. The water phase was acidified to confirm the SBO release from the blend into the water phase by the presence of precipitated material.

Table I. Analytical Data for FORSUD and CV

SBO	Volatile solids (w/w %)a	pH	C (w/w %)a	N (w/w %)a	C/N
FORSUD	84.6	6.4	45.07 ± 0.12	7.87 ± 0.12	5.73
CV	72.1	8.2	38.25 ± 0.09	4.01 ± 0.03	9.54

Mineral elements: Si, Fe, Al, Mg, Ca, K, Na as % w/w;a Cu, Ni, Zn, Cr, Pb, Hg as ppma

	Si	Fe	Al	Mg	Ca	K	Na	Cu	Ni	Zn	Cr	Pb	Hg
FORSUD	0.36 ± 0.03	0.16 ± 0.00	0.78 ± 0.04	0.18 ± 0.01	1.32 ± 0.05	9.15 ± 0.06	0.39 ± 0.01	100 ± 1	27 ± 1	185 ± 4	11 ± 0	44 ± 2	0.23 ± 0.01
CV	2.55 ± 0.01	0.77 ± 0.04	0.49 ± 0.04	1.13 ± 0.06	6.07 ± 0.38	3.59 ± 0.21	0.16 ± 0.01	202 ± 4	92 ± 1	256 ± 1	19 ± 1	85 ± 1	0.15 ± 0.02

C types and functional groupsb concentration as C mmol/g of product

	Af	NR	OR	OMe	OCO	Ph	PhOH	PhOY	COOH	CON	C=O	Af/Ar	LH
FORSUD	16.1	3.7	3.7	1.5	1.1	3.7	0.75	0.37	2.6	3.4	0.37	3.3	9.3
CV T230	11.8	2.2	4.4	0.0	1.3	4.1	1.6	0.64	3.8	0.32	1.5	1.8	3.6

a Concentration values referred to dry matter: Averages and standard deviation calculated over triplicates.
b LH = liphophilic to hydrophilic C ratio; liphophilic C = sum of aliphatic (Af), aromatic (Ph), methoxy (OMe), amide (CON), ammine (NR), alkoxy (RO), phenoxy (PhOY), and anomeric (OCO) C atoms; hydrophilic C = sum of carboxylic acid (COOH), phenol (PhOH), and ketone (C=O) C; Ar = Ph + PHOY + PhOR.

SBOs Physical Characterization

Prior to processing in the MiniLab extruder (Figure 1), 100 g of SBO were ground for 3 min with a two blades electric grinder, then they were characterized for their grain size distribution by sieving according to DIN 66165 and ASTM C136 procedures. The sample dry sieving was carried out with a sieve column attached to a screening machine. The column contains seven screens with mesh sizes decreasing from >1.25 mm to <0.04 mm from the top to the bottom screen. The screening machine applies to the column a swinging horizontal movement every 10 min. When performing the sieve analysis, the sample is put onto the biggest screen and fractionated into particles of different sizes as the column feed proceeds from one screen to the other. The grain size distribution of the sample is determined by weighing the remnants on each single screen. For the SBO, the analysis was performed on 50 g samples. The smallest parts were analyzed with a Nikon SMZ1500 zoom stereomicroscope (Nikon Instruments) and the size values were acquired through a Nikon camera and the NIS-Elements software.

Molar Mass Distribution

The molecular characterization of the EVOH–SBO blends was performed by means of a size exclusion chromatography (SEC)–multi angle static light scattering (MALS) system using N,N-dimethylacetamide (DMAc) organic solvent as SEC mobile phase, under the following experimental conditions: chromatographic system: GPCV2000 + MALS + DRI; columns set: 2 PLgel Mixed C Polymer Laboratories; mobile phase: DMAc + 0.05M LiBr; temperature: 80°C; flow rate: 0.8 mL/min; sample concentration: ≈3 mg/mL.

Infrared Spectroscopy

Fourier transform infrared (FTIR) spectra in attenuated total reflectance (ATR) mode were performed on a Nicolet 5700 (Thermo Electron Corporation) spectrophotometer equipped with DTGS detector and working with 16 scans at 4 cm^{-1} of resolution in the 4000 to 400 cm^{-1} range. The spectra were obtained directly on the flat surface of samples collected from the Minilab compounder.

Thermogravimetric Analysis (TGA)

TGA of the samples was performed with a Shimadzu TGA-50 (Japan) analyzer. Dynamic analysis was conducted in air at a heating rate of 5°C/min, from 20 to 800°C. Weight loss measurements as a function of temperature were performed from 8 mg samples.

Differential Scanning Calorimetry (DSC)

DSC measurements were performed using a Mettler Toledo (Switzerland) DSC1 calorimeter under nitrogen flow. About 15 mg of sample were inserted inside hermetic aluminum sample pans. A first heating ramp at 10°C/min from 0°C to 200°C was performed to erase sample thermal history. After 2 min at 200°C, the cooling ramp to 0°C at 10°C/min was started. The sample was then kept 2 min at 0°C. Afterward, a second heating cycle, similar to the first one, was carried out. The glass transition (T_g), cold crystallization (T_c), and melting (T_m) temperatures were determined. The T_g value was taken as the midpoint of the DSC heating curve deflection from baseline. Enthalpy values were determined by integrating the area of the cold crystal-

lization and melting peaks. The crystallinity degree (χ_c) for each blend was calculated according to eq. (1):

$$\% \chi_{c1} = 100\Delta H_m/(w\Delta H^{\circ}_{m1}), \quad (1)$$

where ΔH_m is the melting enthalpy of the blend sample (J/g), ΔH°_{m1} is the melting enthalpy (169.2 J/g) of the EVOH sample assuming 100% crystallinity as in pure polyvinyl alcohol (PVOH),[11] and w is the EVOH mass fraction in the composite

X-ray Diffraction (XRD)

XRD patterns were obtained directly on the surface of the polymeric samples using the diffractometer PW3040/60 X'Pert PRO MPD from PANalytical, in Bragg-Brentano geometry, equipped with the high power ceramic tube PW3373/10 LFF source with Cu anode. The crystallinity index (CrI) is calculated for the different samples according to eq. (2),[12]

$$\%CrI = \frac{I_f - I_s}{I_f} 100, \quad (2)$$

where I_f is the peak intensity of the fundamental band at $2\theta = 20.1°$, and I_s is the peak intensity of the secondary band at $2\theta = 21.2°$. In this fashion, CrI measures the crystallinity of the synthetic polymer only, and it is directly comparable with χ_{c1} value obtained from eq. (1). The CrI is a time-save empirical measure of relative crystallinity,[13] a fast way to compare the XRD results to the grade of crystallinity (χ_c) measured with the most used DSC analysis.

Mechanical Bending Test

Flexural properties were measured with a bending system on a Tinius-Olsen H5KT testing machine. This instrument allowed calculating the flexural strength (or stress) at break and the bending modulus of the extruded blends in Figure 2. The samples' dimensions were 25 mm (length) × 10 mm (width) × 1.5 mm (thickness). For these measurements, the samples were inserted under a crosshead after conditioning at 25°C and 60% relative humidity for at least 1 week. Stress curves versus crosshead displacement were registered by the Tinius Olsen's Horizon software. The crosshead displacement rate was 50 mm/min. Five tests for each sample were conducted. The means of all the parameters were examined for significance by analysis of variance (ANOVA) using the software JMP version 9 (SAS Institute Inc., Cary, NC, USA).

RESULTS AND DISCUSSION

Chemical and Physical Characterization of Neat EVOH and SBO, and Their Blends

The SBOs used in this work were available from previous work.[3,8] They were shown to contain either organic and mineral matter, the latter constituted mainly by silicates containing Ca, Mg, Al, Fe, Na, and K cations present in 15 to 28% concentration relatively to the dry matter content. The organic matter is a mix of polymeric molecules. In this work, the CV and FOR-SUD SBO weight (M_w) and number (M_n) average molecular weights were measured to yield 66 and 188 kDa M_w, and 4.7 and 1.4 dispersity index (M_w/M_n), for the two SBO, respectively. These materials were found to contain aliphatic and aromatic C atoms bonded to a variety of acid and basic functional groups.[3,8] Because of their biological origin, the SBO molecules

Table II. Molecular Weight Associated to Chromatograms' Peaks 1 (Mp1) and 2 (Mp2) in Figure 4, and/or Viscosity Data[a] for Neat EVOH, FORSUD, and CV SBO, and EVOH-SBO Blends with Different SBO wt % Content

Sample ID[a]	Material, SBO content wt %	Molecular weight		Viscosity data[b]	
		Mp1 (kDa)	Mp2 (kDa)	n index	K (Pa s^n)
P	Extruded neat EVOH[c]	24		0.51	1397
A	Neat FORSUD	124.6			
B	Neat CV	45.7			
A1	EVOH-FORSUD, 2%	24.2	137.2	0.62	611
A2	EVOH-FORSUD, 5%	26.9	172.7	0.63	576
A3	EVOH-FORSUD, 10%	28.1	237.7	0.62	602
A4	EVOH-FORSUD, 14%	28.2	307.2	0.65	509
A5	EVOHFORSUD, 17%	29.2	357.1	0.52	1204
A6	EVOH-FORSUD, 29%	34.1	466.0	0.48	1777
A7	EVOH-FORSUD, 41%	58.5	630.1	0.42	2824
B2	EVOH-CV, 5%	23.9	123.7	0.61	658
B3	EVOH-CV, 10%	24.7	135.6	0.56	984
B5	EVOH-CV, 17%	24.7	151.6	0.59	838
B6	EVOH-CV, 29%	27.8	162.9	0.50	1650

[a] Sample identification.
[b] Parameters calculated from eq. ((3); see text).
[c] Obtained by extruding commercial Soarnol as received (see "Experimental" section).

are most likely not homogeneous. The molecular assembly contains C moieties reminiscent of the pristine polysaccharide, protein, and lignin matter present in the starting biowastes as collected, before anaerobic and/or aerobic fermentation. For the two SBOs, Table I reports relative concentration data for several C types and functional groups, which were identified and measured by using 13C NMR spectroscopy, potentiometric titration, and C and N microanalysis. The data show that, compared with FORSUD SBO, the CV SBO obtained from compost contained more aromatic lignin-like matter, acid functional groups, and ash content, and was more hydrophilic. In essence, the aliphatic to aromatic C ratio (Af/Ar) was 3.3 for FORSUD and only 1.8 for CV. The content of acid functional groups, as C mmol per product gram, was COOH 2.6 and PhOH 0.75 for FORSUD, and COOH 3.8 and PhOH 1.6 for CV. The lipophilic to hydrophilic C (LH) ratio was 9.3 for FORSUD and 3.6 for CV. The ash content, as wt % referred to dry matter, was 15% for FORSUD and 28% for CV.

Several EVOH-SBO blends were made by mixing EVOH with different amounts of FORSUD or CV. These were extruded as reported in "Experimental" section. Table II reports the mass composition for each sample, together with molecular weight and rheological data. The blends were characterized first by their FTIR spectra registered in ATR mode to support the presence of the added SBO in the blend. As for the previously reported samples obtained by solvent casting,[3] the FTIR spectra of the extruded blends, compared with the spectrum of the neat EVOH sample, exhibited the EVOH signals and two new signals due to the presence of SBO. The spectral region above 2500 cm^{-1} was dominated by the broad bands arising from the OH stretching vibration covering the 3600 to 3000 cm^{-1} range

and by the bands falling in the 3000 to 2800 cm^{-1} range arising from CH stretching vibrations. These functional groups and C moieties are common to both neat EVOH and neat SBO. On the contrary, the spectral region below 1800 cm^{-1} allowed distinguishing the EVOH from SBO. The neat EVOH polymer exhibited its strongest absorption bands centered at 1460, 1334, and 1140, and 1040 cm^{-1} arising from the vibrations of the C—C, C—H, and C—O—H bonds, respectively, of its molecular structure. The neat SBO exhibited two main rather broad bands centered at 1650 and 1560 cm^{-1}. They arise from the carboxylate and amide C=O stretching vibrations, respectively. These bands were visible only at SBO relative content ≥17%. Figure 3 reports typical spectra for the EVOH/FORSUD blends at 17, 29, and 41% FORSUD concentration, next to the neat EVOH and neat FORSUD spectra. It may be observed that the relative intensity of the three main SBO bands increases upon increasing the added SBO relative content in the blend, as expected. Very interestingly, one can also observe that the relative intensity of the band at 1040 cm^{1}, compared with that at 1140 cm^{-1}, increases upon increasing the SBO relative content in the blend. As the absorption at 1040 cm^{-1} in the spectrum of neat SBO is rather negligible; the rise of the relative intensity of this absorption in the blends spectra may reasonably be expected to results from new C—O—C bonds formed in the reaction of EVOH and SBO. The band position is more consistent with that arising from the spectra of aralkyl ethers falling near 1075 to 1020 cm^{-1},[14] than with that of aliphatic ethers being rather weak. The band at 1040 cm^{-1} could also arise from the symmetrical C—O—C stretching vibration of esters. The intensity of this band is also rather weak. In addition, the spectra in Figure 3 do not allow to assess the presence of the main esters C=O
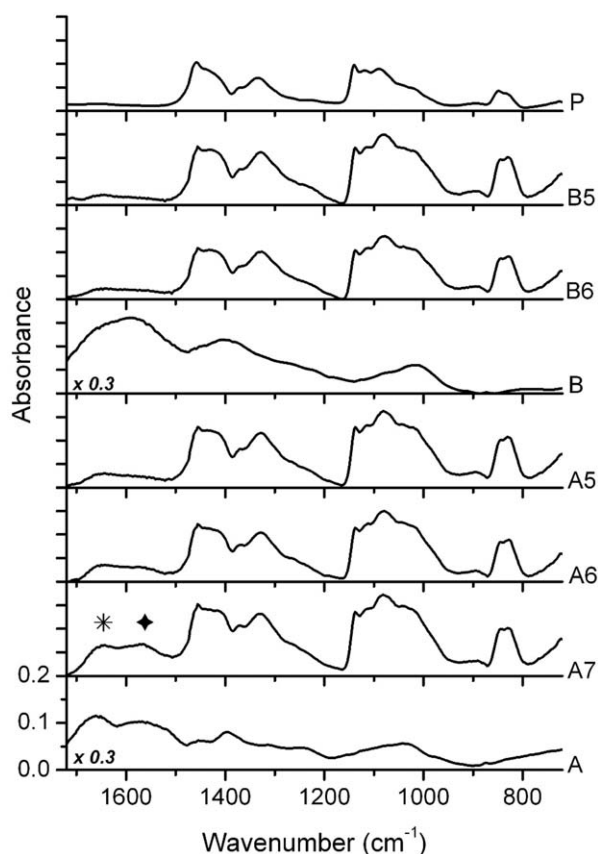
Figure 3. FTIR spectra in ATR mode of neat EVOH (P), neat FORSUD (A), neat CVT230 (B), and of the blends EVOH-FORSUD at 17% (A5), 29% (A6), 41% (A7), and EVOH-CVT230 at 17% (B5) and 29% (B6) SBO content. Star and diamond symbols evidencing the two main SBO signals.

band in the spectral range above 1715 cm^{-1}. The spectra of the EVOH-CVT230 (B, B5, and B6 in Figure 3) exhibit the same features as those of the EVOH-FORSUD blends. The FTIR spectra of both EVOH-FORSUD and EVOH-CVT230 blends therefore suggest the occurrence of a condensation reaction between the EVOH hydroxyl functional groups and the SBO phenol functional OH groups (Table I) with formation of aralkyl ether bonds. No other spectroscopic technique was found suitable to support this reaction. In principle, 13C NMR spectroscopy allows to identify C atoms in a wide variety of organic moieties. However, the 13 C NMR spectra of the neat SBOs are characterized by broad bands covering the entire resonance range from 0 to 200 ppm. Under these circumstances, it is practically impossible to pick a resonance signals that allowed identifying selectively a specific C—O—C arising from the reaction of EVOH and SBO. Confirmation of this reaction was however obtained by selective extraction experiments carried out with aqueous NaOH at room temperature and at 60°C, according to a previous procedure used for the characterization of the EBOH-SBO films obtained by solvent casting.[3] By this procedure (see "Experimental" section), three types of SBO in the blend were identified: that is, (i) SBO not bonded to EVOH, soluble in aqueous NaOH at room temperature; (ii) SBO bonded to EVOH by hydrolysable ester bonds, becoming soluble only upon hydrolysis of the EVOH-SBO copolymer carried out in

60°C NaOH; (iii) SBO bonded to EVOH by not hydrolysable covalent bonds, not released into the alkaline solution even after treatment at 60°C. The same reaction at 60°C is carried out for the extraction of SBO from its sourcing digestate (FORSUD) and compost (CVT230) materials. The results of the above selective extraction procedure showed that only one tenth or two thirds of the starting SBO amount in the EVOH-SBO blends containing 5 and 15% SBO, respectively, is soluble in NaOH, either at room temperature or 60°C. This indicates that most of the SBO contained in the blend is bonded to EVOH with not hydrolysable covalent bonds, such as suggested by IR spectroscopy. The reaction between EVOH and SBO might involve also participation of the mineral fraction present in the SBOs. Assessing the effect of the mineral fraction on the SBO reactivity implies demineralization of SBO and comparing the reactivity of the demineralized SBOs with that of the pristine SBO. Attempts to demineralize SBO by HCl and HF metal ion stripping were found to cause important changes in the residual organic fraction composition relatively to that in the pristine SBO. This pointed out that new biopolymers could potentially be obtained by further acid treatment of SBO. Under these circumstances, further testing of the reactivity of the demineralized SBO with EVOH was planned for being carrying out in future work to comprise the full characterization of both the new acid treated SBO biopolymers and the corresponding blends.

The same reaction between SBO and EVOH was proposed to occur also for the blends prepared by solvent casting,[3] but the IR evidences supporting it were not as clear as in Figure 3. To complete the discussion on the assignment of the band at 1040 cm^{-1} observed in this work, it should be mentioned that previous work[15] has reported for several polyethylene-co-vinyl alcohol polymers FTIR spectra similar to those in Figure 3. In this case, the broad band at lower wavenumber was centered at 1090 cm^{-1}. In addition, the increase of the intensity of the 1140 cm^{-1} relative to that at 1090 cm^{-1} was observed upon increasing the annealing temperature of the sample and appeared related to increasing molecular order along the polymer chain. On the contrary, the decreased intensity of the 1140 cm^{-1} relative to that at 1090 cm^{-1} was assigned to the decrease of the sample crystallinity.[15] In the present case of the EVOH-FORSUD blends, the increase of the intensity of the broad band centered at 1040 cm^{-1} relative to that at 1140 cm^{-1} is associated to increased crystallinity of the blend see (Thermal and XRD Data below).

Molecular weight measurements by SEC-MALS provided additional information on the chemical nature of the blends. The important and very critical problem in the SEC fractionation and characterization of the EVOH-SBO blends was finding an adequate solvent for the neat EVOH and SBO materials, and for their blends. DMAc containing 0.05M LiBr was found a good solvent providing the best compromise between polymers solubility and adequate SEC fractionation. All samples independently of relative content of components were completely soluble in the DMAc-LiBr solvent system at 80°C. No evidence of disperse solid particles or gel or insoluble fractions in the solutions was noted. All solutions were clear and the filtration by 0.20-mm filters was easy without any resistance to the filtration. Furthermore, the experimental calibration from the on-line light
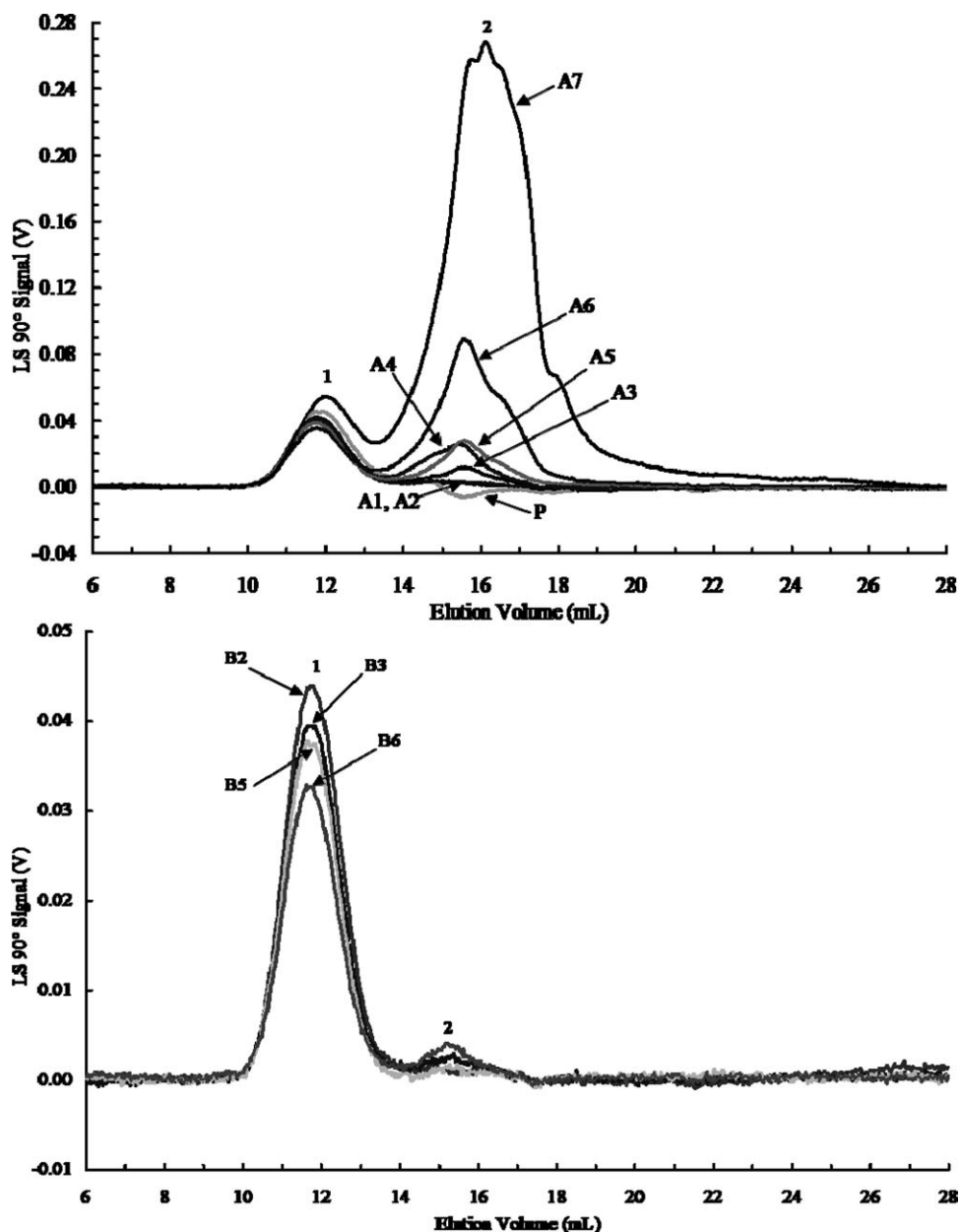
Figure 4. Light scattering signal (MALS 90°) versus elution volume for EVOH and the blends listed in Table II.

scattering detector (MALS) does not show evidence of meaningful aggregation of macromolecules. Substantially all samples were completely soluble in the used experimental conditions without presence of gel and/or meaningful aggregates. The molecular weight of samples was obtained from an on-line absolute MALS detector, not from a relative calibration. Consequently, the estimation of M_n, M_w, M_z, and so on was sufficiently accurate. The molecular weight obtained under these conditions is defined "apparent" because samples are mixtures of the different components and/or copolymers formed from their reaction. Consequently, some fractions could have a complex composition. The important problem in the characterization of such samples is an adequate chromatographic fractionation, more so than solubility. It is important to note that the SEC fractionation under the adopted experimental

conditions was very good and the main components of the blends were sufficiently separated. Overall, the estimation of the molecular weight of samples is accurate, particularly in comparison with the starting components. Figure 4 shows the comparison of the light scattering signal (MALS photodiode 90° angle) versus elution volume for the starting EVOH, and the EVOH-FORSUD and EVOH-CV blends. The comparison of the differential molecular weight distribution (MWD) of the starting components and the blends is shown in Figure 5, that is, the neat EVOH, FORSUD, and CV, and the two blends with low (10% FORSUD and 5% CV) and maximum (41% FORSUD and 29% CV) SBO content. For all analyzed samples, Table II reports peaks' molar mass (M_p) values. It may be observed that each neat material exhibits unimodal MWD. However, the three materials are characterized by different M_p values, that is,
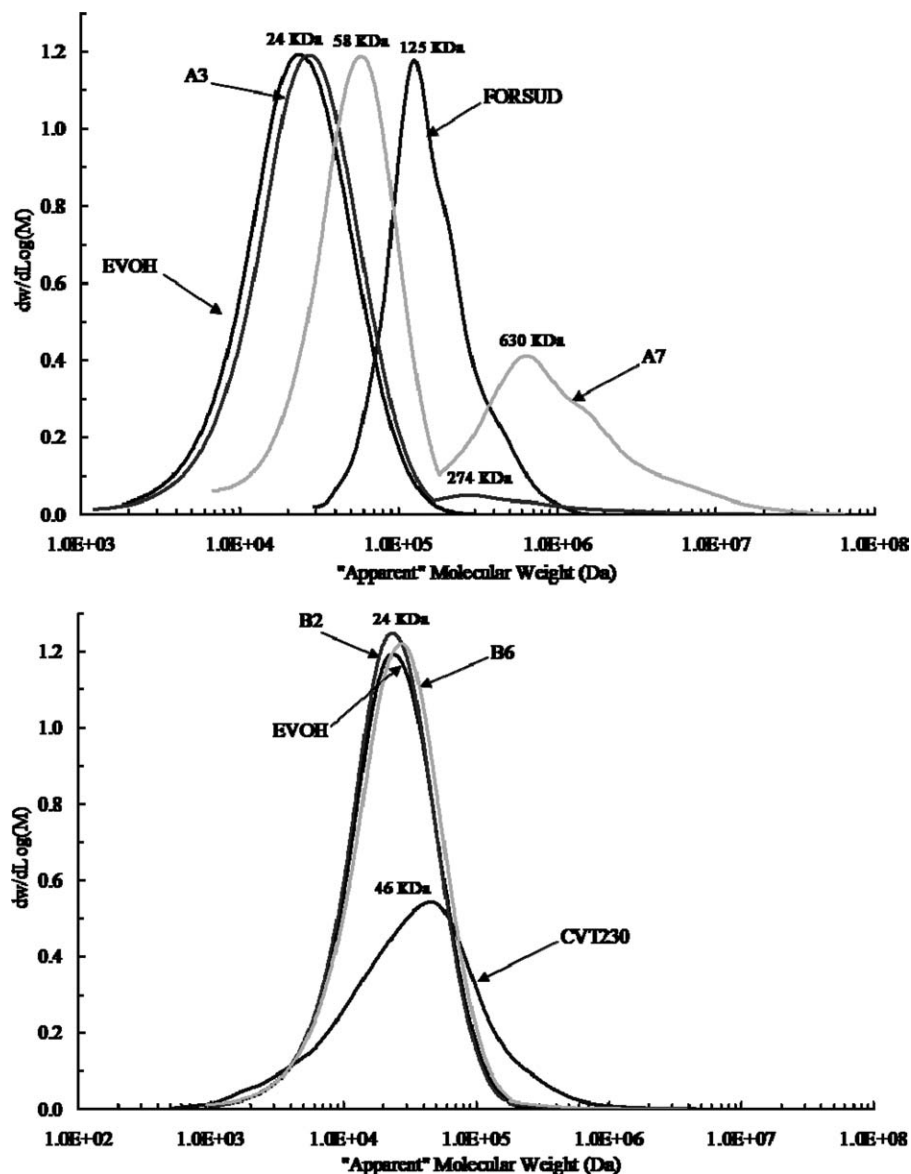
Figure 5. Differential molecular weight distribution versus apparent molecular weight for EVOH, FORSUD, CV, and their blends listed in Table II.

24 kDa for neat EVOH, 46 kDa for neat CV, and 125 kDa for neat FORSUD. On the contrary, the chromatograms of the blends exhibited a bimodal distribution. This was mostly evident for the EVOH-FORSUD blends. Figures 4 and 5 show that the chromatograms of these blends exhibit, for each sample, two relatively separate peaks. The bands associated with these two peaks undergo strong changes in both position and relative intensity. Indeed, the M_p value of the first peak ranges from 24 kDa (pure EVOH) to 58 kDa (blend with 41% of FORSUD), whereas the M_p values of the second peak ranges from 125 kDa (pure FORSUD) to 630 kDa (blend with 41% of FORSUD). In addition, the chromatogram in Figure 4 shows that, upon increasing the FORSUD content, the band area and intensity corresponding to the second peak increase greatly, relatively to the band area corresponding to the first peak. Based on these changes, it can be reasonably hypothesized that the first peak at

lower M_p value results from macromolecules containing EVOH repeating units as major component, whereas the second one at higher M_p value corresponds to a pool of molecules whose composition is dominated by FORSUD material. Under these circumstances, the molecular pools corresponding to the two different peaks, other than the dominating component (EVOH or FORSUD), would contain a minor content of the other component. The data support the belief that a strong interaction occurs between EVOH and FORSUD in the blends. Based on molecular weight data only, it cannot be definitely assessed what type of interaction occurs between EVOH and FORSUD. One could generically make the following two hypothesis: The first peak arises from the formation of clusters or aggregates between EVOH and the lower molecular weight components of the neat FORSUD macromolecular pool for the first peak; the second peak arises from clusters or aggregates formed by the

bigger macromolecules of the neat FORSUD molecular pools and a lower amount of EVOH molecules. However, the FTIR spectra in Figure 3 suggest the occurrence of a chemical reaction between OH groups of EVOH and FORSUD molecules with formation of ether linkages. This reaction could very well be also responsible for the shift of the M_p values observed upon increasing the FORSUD content in the blend.

The molecular weight pattern for the EVOH-CVT230 blends, and its changes upon increasing the CVT230 content, was much different from those for the EVOH-FORSUD blends. Figures 4 and 5 show that, in the case of the EVOH-CVT230 blends, the bimodal MWD is barely visible. Indeed, although Table II reports M_p values for two peaks also for the EVOH-CV blends, the M_p values of the second peak are not accurate because the area of this second peak is minimal. In addition, the shifts of the M_p values and the changes of Figures 4 and 5 distribution patterns of the EVOH-CV blends, upon increasing the CV content, are much smaller than those observed for the EVOH-FORSUD blends. This points out that, although the IR spectra suggest a similar condensation reaction for the two types of blends, the interaction between CV and EVOH is not as strong as that between FORSUD and EVOH. The interpretation of this behavior is further discussed hereinafter taking into account the results of the blends viscosity and thermal measurements, and the previously published results obtained on the solvent cast blends (see Section below: Comparison of the results by extrusion and solvent casting).

Undoubtedly, the analyzed system is very complex, both because of the occurrence of H-bonding interactions and of a chemical condensation reaction between the components, and because of the heterogeneous nature of the biopolymers participating in these interactions and/or reactions. In spite of the above justifications for the adopted experimental conditions and/or interpretation of the results, one could still wander about what is truly analyzed by SEC. A definite unequivocal answer to the question arising from the SEC experimental conditions used in this work requires further dedicated complex analytical work. This was beyond the scope of the present article. As demonstrated below, the result of the SEC fractionation performed in the present work show significant differences between samples that are well consistent with the different viscosity, thermal, and mechanical properties and chemical data obtained for the same samples. Within the scope of the present work, the consistency of all different measurements validates the drawn conclusion on the comparison of the nature and behavior of the blends containing the same components obtained by extrusion and solvent casting. Thus, the significance of the SEC data obtained in this work should not be viewed from a rigorous strictly analytical point of view, but should be rated based on the consistency of the results with those obtained through the other many different measurements and on the support given to the drawn conclusions.

The particle size distribution of the ground SBO powder samples, which were used in the blend preparation, is shown in Figure 6. Optical micrography of the smallest part collected, sum of the total particles with size <0.25 mm (Figure 7), showed a big heterogeneity in particle size and area.
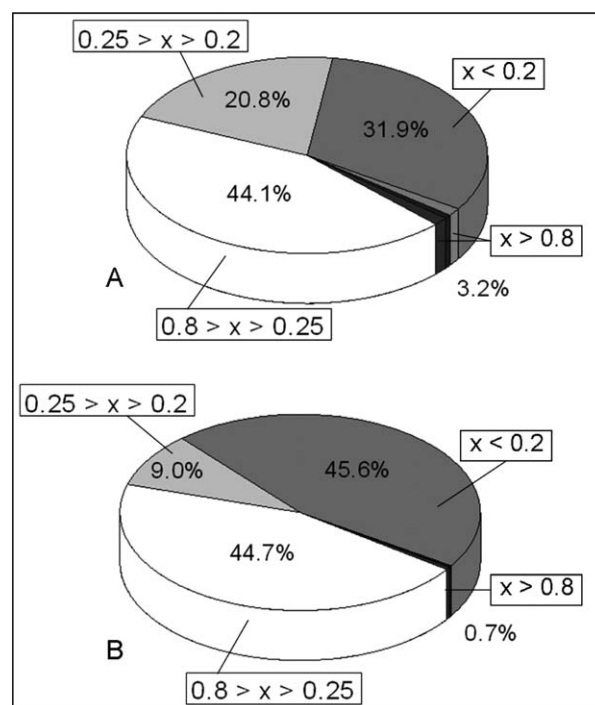

Figure 6. SBOs grain size (diameter, mm) distribution for FORSUD (A) and CVT230 (B).

Viscosity Measurements of Neat EVOH and Blends

The samples collected from the MiniLab compounder revealed increasing color intensity upon increasing the SBO w/w % content in the blend (Figure 2). In the samples prepared at low SBO amount (i.e., at 2 or 5%), a brownish polymeric matrix with a lot of homogenously dispersed brown SBO particles could be observed. Viscosity versus shear rate duplicate measurements were carried out for each blend. The results were very well reproducible as shown from the typical example reported in Figure 8. Viscosity decreased systematically upon increasing the shear rate, thus revealing a rheofluidifying behavior for all blends. For all investigated samples, the experimental data in Figure 8, were fitted with a 0.99 correlation coefficient by the Ostwald–De Waele power-law eq. (3)[16]:

$$\eta = K\dot{\gamma}^{n-1}, \tag{3}$$

where η is the apparent viscosity (Pa s), γ is the shear rate (s^{-1}), K is the consistency (Pa s^n), and n is the power-law index. The n and K parameters calculated from the data fittings are reported in Table II. The results show that neat EVOH and all blends have the same pseudo plastic behavior, that is, $n < 1$. For the blends, the increase in viscosity upon increasing the SBO relative content results either in the increase in K consistency and in the decrease in n index. As a result, flowing of the samples at SBO content >20% was rather difficult. However, the blends with SBO content <20% exhibited lower K and higher n than the neat EVOH sample. SBO thin particles produce exactly the opposite behavior found in a previous work[16] preparing composites, in MiniLab compounder, of poly(lactic acid) and natural fiber. This fact is correlated to the physical nature of SBO used in the composites preparation. Blends with SBO content <20% contained solid SBO particles being well
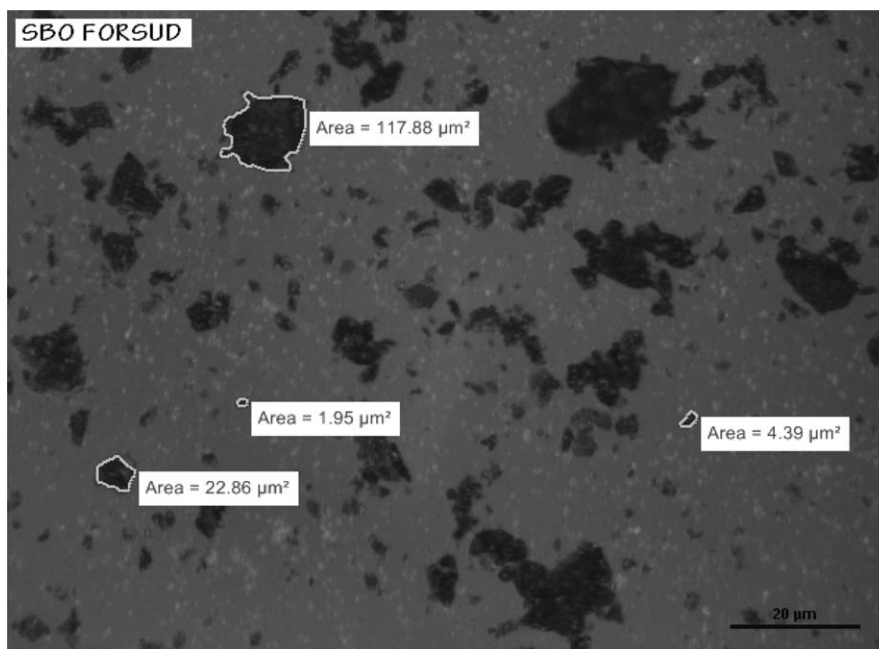
Figure 7. Micrograph of FORSUD smallest fraction with size <0.25 mm.

and better dispersed in the polymer matrix than those of the blends at SBO content >20%. As a result, the blends with SBO content <20% flowed more easily than the neat EVOH and the blends with SBO content >20%, thus revealing lower values for apparent viscosity. Figure 9 depicts this situation for the neat EVOH and all blends at 50 rpm screw rotation speed, that is, only 177 s^{-1} shear rate. At this experimental low shear condition, eventual polymeric degradation reactions[17] are minimized because the sample is kept for 1 or 2 min into the MiniLab chamber. In addition, if the initial particles are initially randomly dispersed in the polymeric matrix, they tend to align themselves with the major axis in the direction of shear, thus reducing the viscosity. The degree of alignment is a function of the deformation rate. At low shear rates, there is only a slight departure from randomness, but at high shear rates, the particles are almost completely oriented. The plots of the data collected at low 177 s^{-1} shear rate (Figure 9) show that, by the addition of small amounts of SBO, the viscosity of the blend decreases below the value for the neat EVOH sample and
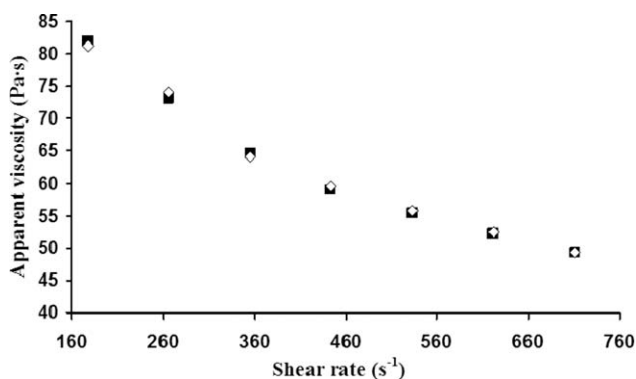
reaches minimum values at 5 to 10% SBO. At higher SBO content, the viscosity increases back to the neat EVOH value (around 15–20% SBO) and reaches much higher values at SBO content >30%. In this scenario, the viscosity of the EVOH-FORSUD blends is lower than that of the CV blends. The data suggest that both SBOs, at low concentration (<20%), reveal a plasticizing effect on EVOH, but the FORSUD is more effective than CVT230. This fact appears related to the stronger interaction of FORSUD with EVOH evidence by the MWD data in Figures 4 and 5.

The viscosity of neat EVOH, as well as its excellent barrier properties to gases, hydrocarbons, and organic solvents, are caused by strong H bonds interactions, both inter- and intra-
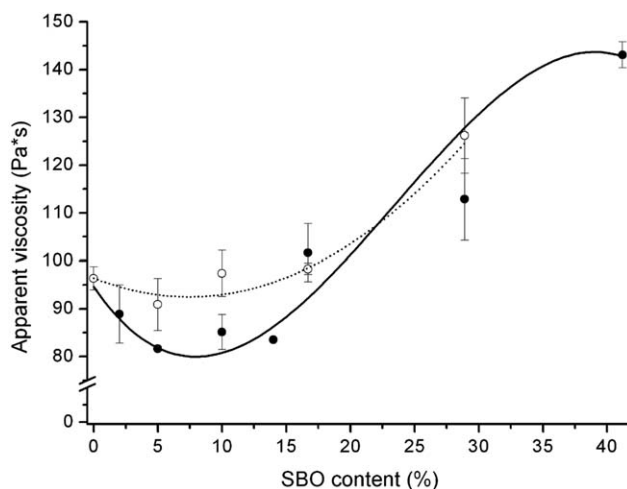

Figure 8. Apparent viscosity versus shear rate from duplicate measurements for the EVOH/FORSUD 5% samples (A2 in Table II).

Figure 9. Apparent viscosity, measured at 50 rpm screw rotation speed (i.e., 177 s^{-1} shear rate), versus SBO content (black circles for FORSUD and white circles for CVT230) in the composites.
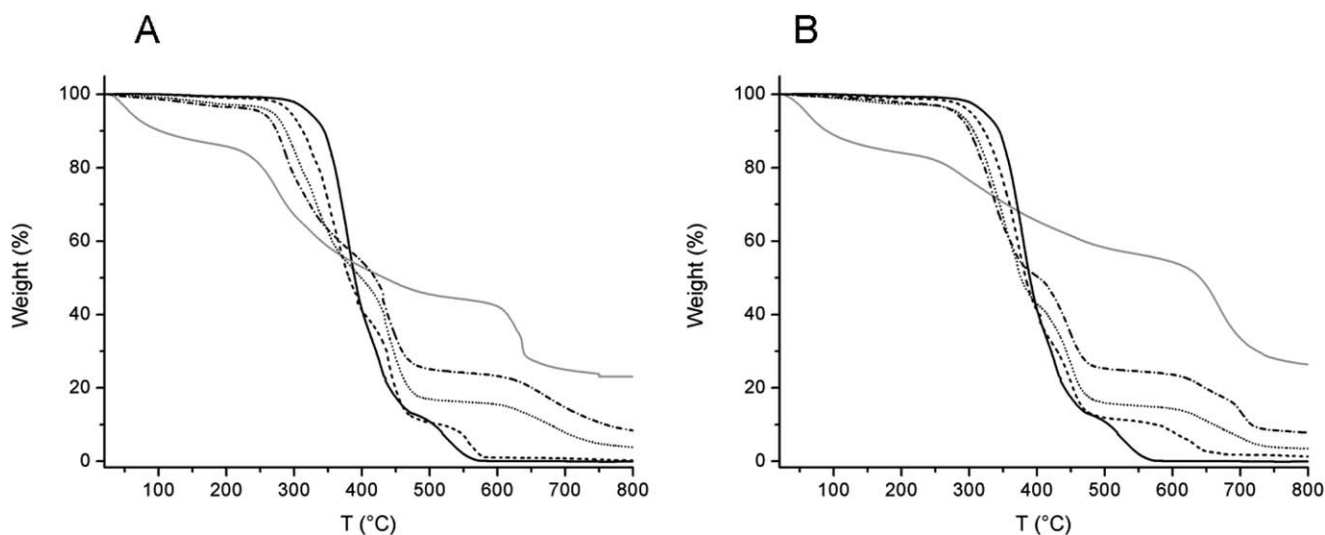
Figure 10. TGA scans reporting sample weight loss % upon increasing temperature for neat EVOH (solid black line), neat SBOs (gray line), and the EVOH blends with FORSUD (A) and CVT230 (B) at three different SBO concentrations, that is, 5% (dashed line), 17% (dotted line), and 29% (dot-dashed line).

molecular. These end up reducing the free volume of the polymer chains.[18] Barrier properties to gases and liquids are of high importance depending on the intended application. Testing the performance of the EVOH-SBO blends in specific applications was not within the scope of the present work. Viscosity as directly related to the blends nature and composition, and indirectly to the product mechanical properties, was deemed more important for a preliminary assessment of the new extruded blends. Indeed, the decrease of viscosity may occur for different reasons. One is the formation of a new copolymer, such as it might occur from the reaction of EVOH and SBO. The new copolymer is likely to acquire a different H bond network, where the free volume of the copolymer chains is higher than in neat EVOH. Similar effect has been reported for maleic anhydride-grafted-polypropylene (PPgMA),[18] that incorporated into neat polypropylene causes a reduction of the viscosity. Other factors lie in the ability of SBO to dissolve in the EVOH matrix. In this case, two possible interactions may be envisaged, that is, electrostatic or H-bonding interactions. In the former case, the smallest SBO particles with almost spherical shape (Figure 4) may occupy the space between polymeric EVOH molecules, increasing the EVOH intermolecular distance and so permitting higher mobility of the EVOH molecules. Spherical particles that flow and disperse well through the molten polymer matrix cause the least problems related to stress concentration.[18] The filler particles make them able to slide within the EVOH system during application of shear forces causing a flow-favoring orientation, which subsequently lower the viscosity of the EVOH matrix. In the latter case, the spacing out of the EVOH molecules may be realized through the formation of new hydrogen bonds between SBO functional groups and EVOH alcoholic groups, replacing the intermolecular H bond interactions between the OH groups of the neat EVOH polymer and thus illustrating the plasticizing effect of both SBOs on EVOH. In this case, the increase of the blend viscosity at SBO content >10% may be explained with the saturation of the EVOH OH

functional groups engaged in H-bonding interaction with the added SBO molecules. When this occurs, there are no available EVOH OH groups to interact with further added SBO molecules. Thus, the excess SBO molecules will tend to behave as a filler inside the polymeric matrix and even to aggregate themselves. This may imply higher degree of chain entanglement by H-bonding or physical crosslinking causing a reduction of molecular mobility,[18] and thus viscosity increase. The viscosity versus SBO content plots in Figure 9 more or less indicate a plasticizing effect on EVOH and, possibly, a reticulation at high SBO loading. As the samples at high SBO loading showed poor mechanical properties, further investigation assessing reticulation did not seem worthwhile within the scopes of the present work. On the contrary, it was more interesting to observe the effects of the different types of SBO on viscosity. Indeed, it is known that generally, when the blend viscosity increases relatively to that of the neat polymer matrix, the particles of the filler perturb the normal flow of the neat polymer molecules. In this fashion, the filler ends up hindering the mobility of chain segments in the flow.[19] Under these circumstances, the capacity of the FORSUD SBO to lower the neat EVOH matrix viscosity, more than the CV does, is likely to be connected with the higher molecular weight and more aliphatic structure of FORSUD, compared with the more aromatic rigid lignin-like structure of the CV SBO. Indeed, higher molecular weight may provide higher number of contacts between EVOH and FORSUD, whereas addition of rigid molecules reduces the system flexibility, and thus increase viscosity.[17,18] These feature may contribute a better interaction between FORSUD and EVOH and higher molecular structure flexibility in the EVOH-FORSUD blends than for the EVOH-CV ones. This fact appears indirectly substantiated by the molecular weight data in Figures 4 and 5.

Thermal and XRD Data

Figure 10 reports the TGA scans in air for neat EVOH, the neat SBO samples, and the different blends. It shows that neat
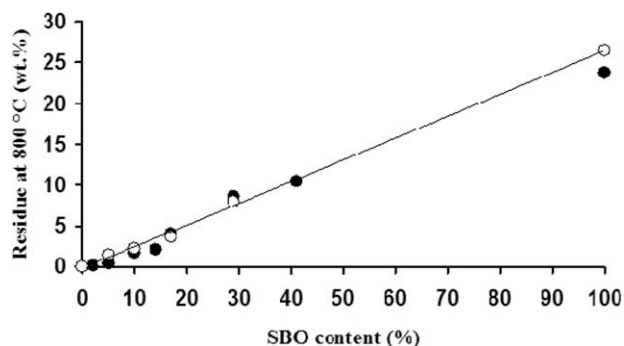
Figure 11. Weight % residue at 800°C for the extruded blends versus added SBO content in the blend preparation (black circles for FORSUD and white circles for CVT230).

EVOH undergoes extensive thermo-oxidative degradation in two successive stages. In the first one, occurring in the 350 to 460°C range, about 85% weight loss is attained. The residual weight loss, up to 100%, occurs between 460 and 550°C. The SBOs show first the loss of adsorbed water upon heating to 150°C, then a gradual weigh loss upon heating to 800°C. In the 150 to 800°C range, two important weight losses occur at 450°C and at 650°C due to the degradation of the SBO organic structure. The residual matter at 800°C corresponds to the SBO ash content. In the blends' scans, it is possible to notice that increasing the SBO content, the thermogram becomes more similar to that of the neat SBO, and that the residual weight at 800°C consequently increases. The modification observed in the onset temperature of the first EVOH thermal degradation stage could be an indication of SBO grafting on EVOH. Such reticulation was already mentioned in a previous work[3] consisting in producing similar blends using the solvent cast technique, a chemical reaction occurring during the blend production, thus resulting in SBO molecules covalently bonded to the EVOH ones. Moreover, for the extruded blends, the blend residue correlates well with the amount of added SBO in the blend preparation. The linear correlation coefficient of the data reported in Figure 11 is 0.99. The weight residue at 800°C can therefore be taken as an indirect probe of the content of SBO in the blend. The TGA data well support the blend composition data given in Table II, which are based on the weighed amounts of the hand-mixed components prior to extruding the blend material.

Figures 12 and 13 report the data obtained from the DSC scans of neat EVOH and the EVOH-SBO blends. The plots of the melting (T_m), cold crystallization (T_c), and glass transition (T_g) temperatures versus the SBO content in the blend show a similar trend as the apparent viscosity versus SBO concentration plots in Figure 9. Relatively to neat EVOH, the blends with 2 to 14% SBO exhibit lower T_m, T_c, and T_g values, whereas at higher SBO content ($>15\%$) they exhibit nearly the same values of neat EVOH. Compared with neat EVOH, the decrease in T_m and especially in T_g observed for the lowest SBO contents (until 14%) illustrates again the plasticizing effect of SBOs on EVOH, as previously observed for viscosity measurements. Similar effects on T_m, T_g, and viscosity are reported for other cases. For example through the incorporation of maleic anhydride-graft-polypropylene in polypropylene matrix.[18] In the specific case of
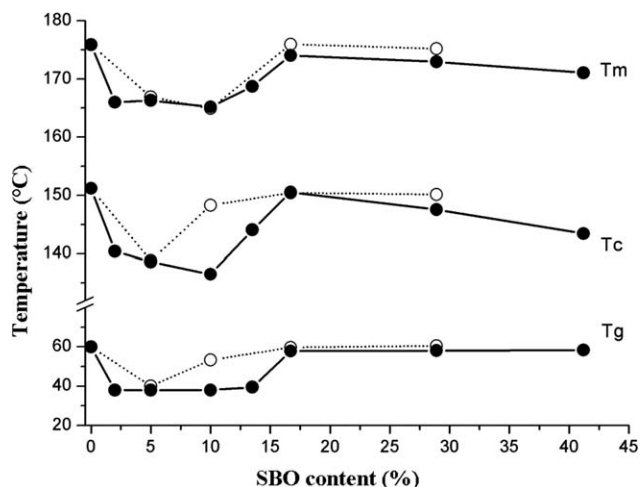

Figure 12. Temperature graph from DSC analysis versus SBO content for all composites (black circles for FORSUD and white circles for CVT230).

the present work, the FORSUD plots compared with the CV plots indicate that the effect of lowering the EVOH T_m, T_c, and T_g by the FORSUD addition is greater than that exhibited by the added CV SBO. This is consistent with the rheological measurements reported in Figure 9 where the decrease in the viscosity is shown more important for FORSUD than for CV with SBO contents of 5 and 10%.
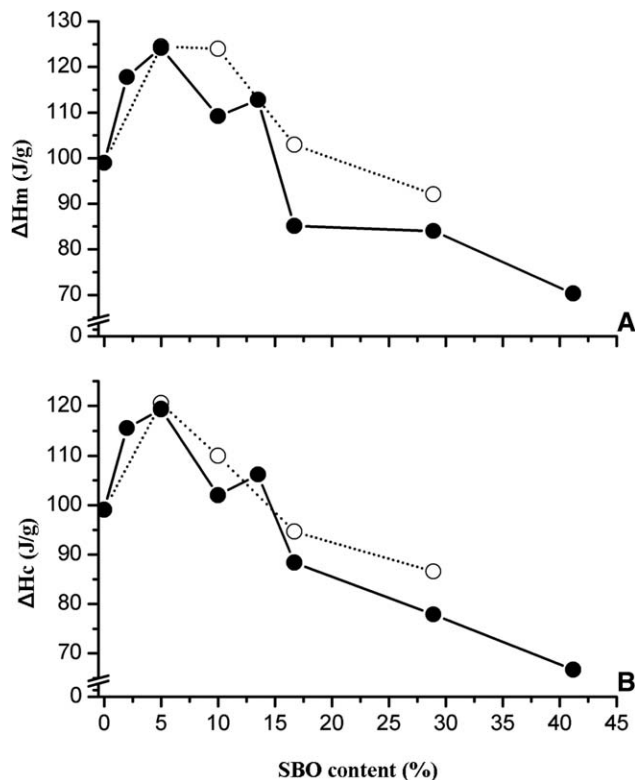

Figure 13. Melting (A) and cold crystallization (B) enthalpy graph from DSC analysis versus SBO content for all composites (black circles for FORSUD and white circles for CVT230).
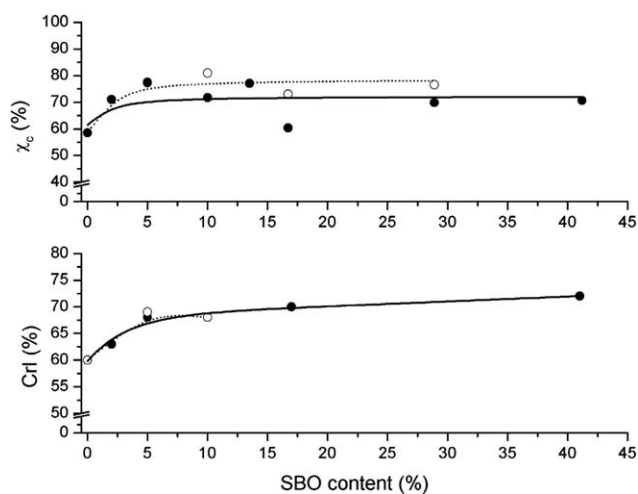
Figure 14. Crystallinity percentage versus SBO content weight % in EVOH-SBO extruded samples (black circles for FORSUD and white circles for CVT230), calculated from melting enthalpies according to eq. (1) and from x-ray diffractograms according to eq. (2; CrI).

Very interestingly, compared with the T_m, T_c, and T_g plots in Figure 12, the plots of the melting (ΔH_m) and cold crystallization (ΔH_c) enthalpies in Figure 13 show opposite trend. In essence, low amounts of SBO (2–10%) increase the enthalpies to a maximum value. These then decrease, upon addition of more SBO, to values much lower than that of neat EVOH. Figure 14 reports the crystallinity percentage calculated from the melting enthalpy values according to eq. (1) and from X-ray diffractograms according to eq. (2; see "Experimental" section). For both rates (i.e., χ_c and CrI, respectively), it may be observed that, upon increasing the SBO content, the crystallinity of the synthetic polymer in the blend increases to an asymptotic value. The excess SBO, that is, more than 10 to 15%, has no further effect on the blend crystallinity.

The changes of phase transition temperatures and specific enthalpies observed for the EVOH-SBO extrudates are quite different than those reported for the same blends obtained by solvent casting[3] (see "Introduction" section). Changes in polymer melting temperature and melting enthalpy, because of different processing conditions, do not always go into the same direction. For example, different PVOH fibers show different melting enthalpies, all higher than the enthalpy value for PVOH in chips form.[2] In these cases, the melting enthalpy increase goes along with the increase of the melting point. For PVOH/starch composites lower melting temperature and lower enthalpy than for pure PVOH has been observed.[20] The decrease in melting temperature coupled to the increase in specific melting enthalpy has been reported for polyolefin/wax and/or natural fibers blends upon increasing the filler content in the blend.[21] In this case, the increase of the blend enthalpy was attributed to several reasons such as (i) the higher specific enthalpy of the added filler compared with the polyolefin (polypropylene and polyethylene) matrix, and (ii) partial miscibility or co-crystallization of the added filler with the polyolefin matrix. On the contrary, the decrease in the specific melting enthalpy of the blend by the addition of a different filler was attributed to inhibition of

the polymer matrix crystallization by the filler acting as plasticizer. For the specific case of the EVOH-SBO blends, two different trends of thermal transition temperatures and enthalpies are observed. For the blends obtained by solvent casting,[3] the ΔH_m decreased, no change in T_m occurred, T_g increased, and T_c decreased upon increasing the SBO relative content. The data reported in the present work for the extruded EVOH-SBO show that, upon increasing the SBO relative content, all thermal transition temperatures decrease, while ΔH_m increases. Compared with the above PVOH, polyolefin, and solvent cast EVOH-SBO blends, the behavior of the extruded EVOH-SBO blends appears rather peculiar. While in the case of polyolefin/wax composites, the decrease of melting temperature and the increase of melting enthalpy observed upon increasing the filler content in the blend could be related to the lower melting temperature and higher specific enthalpy of the filler, in the case of the extruded EVOH-SBO blends, the SBO is a non-melting amorphous filler. Under this circumstance, one would expect a behavior similar to that observed for the EVOH-SBO blends obtained by solvent casting. On the contrary, for the extruded blend, it appears that the amorphous filler, present at 2 to 14% relative content, increases the blend crystallinity.

Looking for possible reasons of the enhanced specific enthalpy caused by the addition of SBO to the EVOH matrix, the extruded blends were analyzed by XRD. Figure 15 depicts the XRD patterns for neat EVOH, neat CVT230, being similar to that of FORSUD, and the EVOH-SBO blends at different compositions. The EVOH copolymers[22] are known to be crystalline irrespectively of composition. They show a polymorphic behavior depending on composition and thermal treatment. The copolymers with relatively high vinyl alcohol content (68–71%), such as the Soarnol copolymer used in the present work, crystallize from the melt into a monoclinic or orthorhombic lattice, depending on the cooling rate. The two lattices give similar patterns, that is, a fundamental high intensity band at 20° 2θ and a smaller band at 21° to 22° 2θ. However for the monoclinic lattice the fundamental band is split into two well distinct signals, falling at 19° to 20° and at 20° to 21° 2θ, respectively. For the orthorhombic lattice, these signals collapse into one broad band. These copolymers crystallize in the monoclinic lattice upon slow cooling, and in the orthorhombic lattice upon quenching. The degree of crystallinity determined from the XRD patterns has been found in the quenched specimens considerably smaller than that in the slowly crystallized samples, standing in contrast to the constancy of the enthalpy of melting. Moreover, no difference in the melting temperatures and enthalpies between the two crystalline modifications has been observed.

For the semicrystalline EVOH copolymer used in the present work, Figure 15 shows sharp well-defined and broad peaks due to small crystallites. In agreement with literature data,[23] the peaks are centered at 10.8°, 20.1°, and 21.2° 2θ. The broad fundamental band at 20.1° 2θ resembles that reported for the copolymer crystallized in the orthorhombic lattice.[22] In contrast, the patterns for the SBOs, as exemplified by that for CVT230 reported in Figure 15, have very broad features consistent with incoherent scatter from an amorphous solid. Figure 15 also shows that, in all analyzed blends, the characteristic EVOH
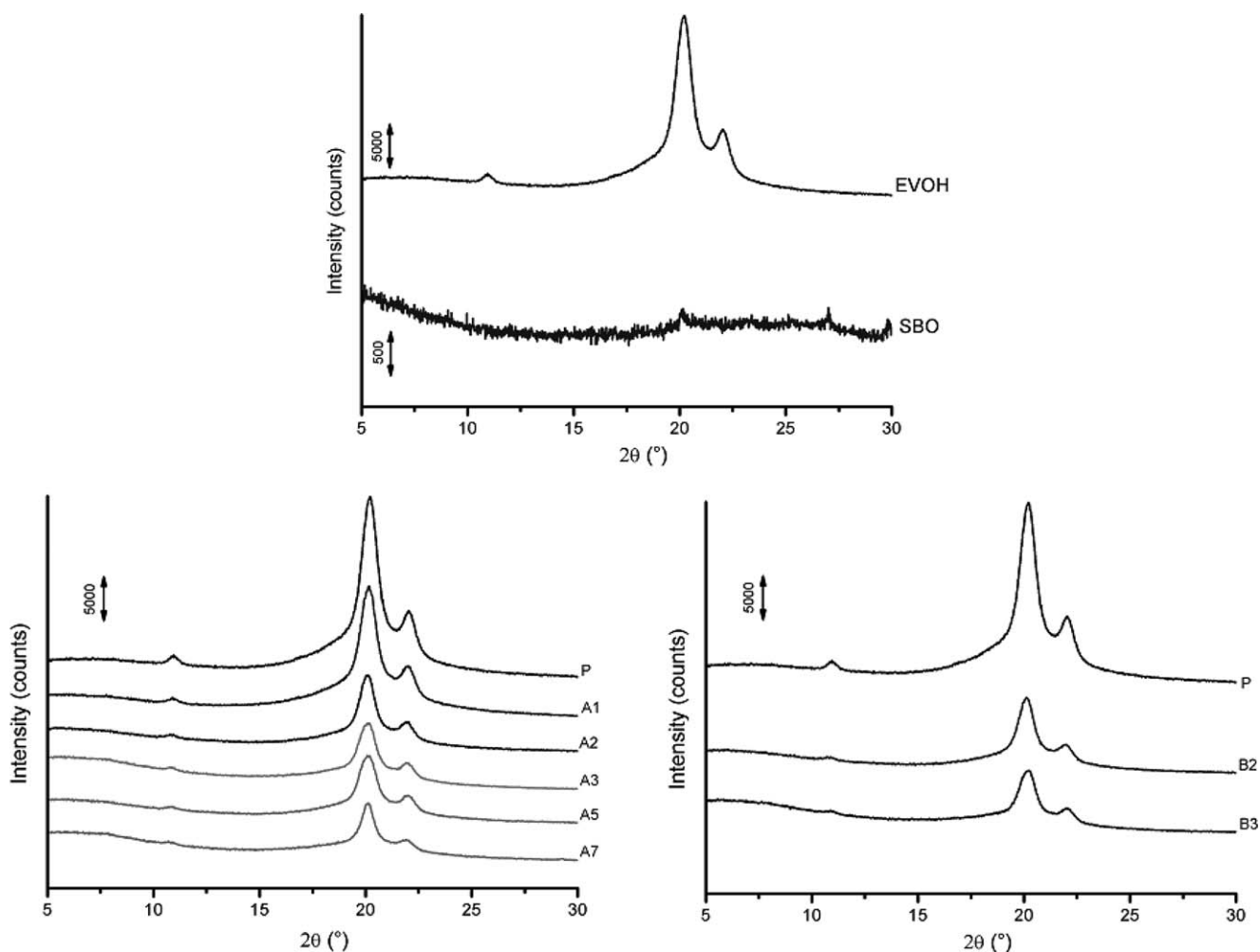
Figure 15. X-ray diffraction patterns for EVOH as received, and for the extrudates obtained in this work, that is, EVOH (P), and the EVOH/FORSUD and EVOH/CV blend samples identified as in Table II.

peaks are maintained in the same position as those for the neat EVOH extruded sample (i.e., sample P). However, upon increasing the SBO content in the blend, the EVOH pattern relative intensity decreases as the broad and spread SBO diffraction pattern in the 5° to 10° 2θ range becomes more evident. In the blends, the two XRD patterns, for EVOH and for the SBO, seem additive. No new signal arising from a new crystalline phase is observed. However, the relative intensity ratio of the signal assigned to the EVOH copolymer changes considerable upon increasing the SBO content in the blend. This change is reflected in the results obtained by eq. (2), which are plotted in Figure 14. Indeed, eq. (2) is based on the relative intensities of the fundamental and the secondary diffraction bands. It accounts only for the relative changes of the synthetic polymer bands, and not for the decrease of the intensity of the synthetic copolymer bands due to the increase of the SBO amorphous fraction pattern intensity. This latter is quite difficult to calculate from the diffractograms shown in Figure 15. Under these circumstances, eq. (2) was used to estimate the change of crystallinity of the synthetic polymer matrix only. Equations (1) and (2) are well consistent with the results shown in Figure 14. These show that the XRD estimation of the degree of crystallin-

ity of the synthetic copolymer matrix is in very good agreement with the results obtained from eq. (1) based on DSC data. In essence, both eqs. (1) and (2) confirm the trend of the synthetic copolymer matrix to acquire higher crystallinity up to an asymptotic value, upon increasing the SBO content in the blend. It seems that the reaction of EVOH and SBO, at SBO relative concentration in the 2 to 15% range, produced a new polymer where the amorphous SBO molecules are grafted to the EVOH molecules. The new polymer is characterized by the same XRD reflection bands as the pristine EVOH, but is crystalline. Amounts of SBO in excess of 15% will not react any further with the synthetic copolymer. They are more likely to produce amorphous SBO aggregates. Because of the spacing out of the EVOH molecules brought by the grafted SBO molecules, and/or by the SBO aggregates, the blend exhibits different T_g, T_m, T_c, and ΔH_m values from the original neat EVOH.

Blends Mechanical Behavior

The flexural strength at break and the bending modulus of the extruded EVOH-SBO blends shown in Figure 2 were measured to investigate the effect of the SBO addition on the blend mechanical properties compared with neat EVOH. The results

Table III. Bending Modulus and Flexural Strength at Break for EVOH-SBO Blends

Sample ID[a]	Material, SBO content wt %	Bending modulus[b] (GPa)	Flexural strength at break[b] (MPa)
P	Extruded neat EVOH[c]	3.9 ± 0.3 a	118 ± 5 a
A1	EVOH-FORSUD, 2%	3.3 ± 0.2 a,b	113 ± 8 a
A2	EVOH-FORSUD, 5%	3.0 ± 0.3 b,c,d	101 ± 17 a,b
A3	EVOH-FORSUD, 10%	3.0 ± 0.3 b,c,d	98 ± 6 a,b
A4	EVOH-FORSUD, 14%	2.6 ± 0.1 c,d	90 ± 3 b,c
A5	EVOH-FORSUD, 17%	3.2 ± 0.3 a,b,c	74 ± 6 c,d
A6	EVOH-FORSUD, 29%	2.8 ± 0.5 b,c,d	57 ± 7 d
A7	EVOH-FORSUD, 41%	3.1 ± 0.1 b,c,d	57 ± 4 d
B2	EVOH-CVT230, 5%	3.1 ± 0.2 b,c,d	102 ± 9 a,b
B3	EVOH-CVT230, 10%	3.0 ± 0.2 b,c,d	88 ± 7 b,c
B5	EVOH-CVT230, 17%	2.5 ± 0.2 d	59 ± 2 d
B6	EVOH-CVT230, 29%	2.7 ± 0.2 b,c,d	55 ± 3 d

[a] Sample identification.
[b] Values are means of quintuplet measurements ± standard deviation; values followed by different letters, in each column are significantly different ($P \leq 0.05$; Tukey tests), that is, a > b > c > d.
[c] Obtained by extruding commercial Soarnol as received (see "Experimental" section).

are reported in Table III. It may be observed that the addition of SBO to EVOH determines a gradual decrease in flexural strength at break and bending modulus compared with neat EVOH. The effect is a little bigger by the addition of CV than FORSUD. From the measurements' mean values and standard deviations, it may be observed that, relatively to neat EVOH, the apparent decrease of flexural strength at break by the increasing FORSUD content up to 10% and by the CV content up 5% is not statistically significant. For the bending modulus, the values obtained for the blends containing up to 17% FORSUD are barely or not significantly different from the neat EVOH's value, while the values for the CV blends appear significantly lower than that for the neat EVOH sample, but not significantly different from those of the FORSUD blends at the same SBO content. The lowering of both flexural strength at break and bending modulus of the blends, compared with neat EVOH, may occur for different reasons. One reason can be expected from the plasticizing effect of the added SBO causing also T_m, T_g, and viscosity decreases because of the EVOH molecular chains free volume increase.[18] Another reason could be the lack of chemical affinity between EVOH and SBO, thus leading to a quite unstable interface. To increase the stability of the EVOH-SBO interface, further studies would be necessary. The possible future addition of judiciously chosen compatibilizers (i.e., coupling agents) inside the EVOH-SBO blends should better the interaction between SBO and the polymeric matrix, and consequently the blend mechanical capacity. The last reason may stem from flow instability. This occurs when, during processing in the melt state, the polymer molecules reach their elastic limit of storing energy, thus causing melt fracture as a way of releasing stress either at the die wall or at the die entrance. In this situation, a rapid and random movement of the oriented molecules in the melt may cause disordered configuration, which allows deformation to take place. For polypropylene/kaolin composites, this phenomenon has been reported to manifest in form of blisters on the surface and void in the cross-section

of the extrudates.[17] Indeed, bubbles were occasionally visible in some of the EVOH-SBO extrudates. One reason for bubbles formation on the extrudate surface has been proposed to be the increasing reduction of the activation energy barrier due to the filler particle/polymer matrix molecule interface occurring as more filler is incorporated in the polymer matrix. Consequently, less force is required to overcome the activation energy barrier, resulting in the formation of more bubbles on the extrudate surface. The sudden pressure and temperature drop of the melt may reinforce this phenomenon during the emergence of the extrudate at the die exit. In these circumstances, the surface layer of the extrudate will solidify first, while the inner layer is still in the molten stage. Soon after, as the inner melt cools down, it will be attracted to the cooled skin of the extrudate layer. Thus, a void forms in the composite extrudate since the total composite volume reduces with time as the temperature gradient drops. Flow instability is triggered whenever processing conditions are not optimized. In the case of the EVOH-SBO blends, this phenomenon requires optimizing the processing temperature and pressure, and the die and flow geometries. In addition, different trends of mechanical strength versus SBO content in the blend may results from extruding the samples in different forms, such as sheet and blown films.

Comparison of Results by Extrusion and Solvent Casting

The results obtained in this work on the extruded EVOH-SBO blends, compared with those obtained in previous work[3] on similar blends obtained by solvent casting, confirm that a chemical reaction during the blend fabrication occurs between EVOH and the SBO. The reaction is likely to involve the hydroxyl groups of the two components with formation of a new copolymer I containing SBO molecules covalently bonded to EVOH molecules:

$$n\text{EVOH} + \text{SBO(OH)} \Rightarrow (\text{EVOH})_{n-1}\text{EV-O-SB} + \text{H}_2\text{O}.$$

In the case of the EVOH-SBO extrudates, the IR spectra in Figure 3 and the selective extraction experiments well support

this reaction. The IR spectra show a new band arising from C—O—C bond stretching vibration, presumably involving either EVOH or SBO C. The selective extraction experiments confirm the presence of water insoluble SBO in the extrudate, which does not leach out in hot alkali. In the case of the solvent cast blends, the assignment of the above IR band to the new copolymer I could not be definitely established, due to the presence of residual DMSO absorbing at the same wavelength. However, selective extraction experiments proved that also the solvent cast films contained water insoluble SBO, which does not leach out in hot alkali. Evidence of this reaction has been obtained in both extrudates and solvent cast films by the MWD of the blends. In the case of the solvent cast blends containing 5.9% FORSUD,[3] only one peak was observed in the SEC chromatogram corresponding to M_p almost three times greater than that of neat EVOH. Samples with higher FORSUD content were not analyzed. In the case of the herewith reported EVOH-FORSUD extrudates, obtained over a much wider range of relative compositions, a second peak is barely visible in the 5% FORSUD sample, but becomes well evident in the 10% FORSUD sample (Figures 4 and 5). The data for the extrudates in Table II show that, upon increasing the FORSUD content, the first peak M_p increases from 24.2 to 58.5 kDa, while that of the second peak increases from 137.2 to 630.1 kDa. These results appear consistent with the blend viscosity data in Figure 9. Indeed, the increase of the molecular weight of the first SEC chromatographic peak could be explained according to the reaction leading to the copolymer I, where the pristine EVOH molecular chains are spaced by the grafted FORSUD molecules. The increase of the molecular weight of the second chromatographic peak might stem from the reaction occurring mostly among SBO molecules with a minor amount of EVOH molecules. This would lead to a second copolymer II containing cross-linked FORSUD and EVOH molecules with the former being in excess over the latter ones. The relative amount of the copolymer II would increase upon increasing the FORSUD content in the starting EVOH-FORSUD mix to be extruded. At low FORSUD content, the formation of copolymer I as major component would be responsible of the decrease of blend viscosity. At high FORSUD content, the high relative content of copolymer II would be responsible of the blend viscosity increase. The formation of the two copolymers I and II, containing mostly EVOH or mostly FORSUD, respectively, had been also proposed for the solvent cast EVOH-SBO blends.[3] The data in Figures 4 and 5 suggest that the interaction between EVOH and CV is not as strong as between EVOH and FORSUD. Consistently with this fact, the effects observed on the melt viscosity (Figure 9) and mechanical properties (Table III) of the blends, caused by the presence of the two SBOs, were significantly different. Compared with CV, FORSUD, by virtue of its stronger interaction with EVOH, up to 10% content, caused a stronger decrease of the blend viscosity and no significant lowering of bending modulus and flexural strength at break. This fact raises another important question on the different affinity of the two SBO versus EVOH. Considering the data in Table I, the better affinity of FORSUD versus EVOH might be related to the higher relative content of aliphatic C, compared with CV. On the other hand,

the higher content of PhOH groups should have favored the chemical reaction for the formation of the copolymer I containing the SBO molecules grafted to the EVOH molecules. The chemical nature and composition of the SBO is too complex to draw definite conclusions based on the available data. Certainly, the investigation of blends with other SBO with different composition,[8] might help to assess the reason for the different affinity versus the EVOH molecules. Aside from the fact that this offer scope for further intriguing research work, the available data demonstrate that both FORSUD and CV blends can be extruded. Therefore, further product development can be carried out by extrusion.

The possibility to fabricate different materials by different technologies, starting from the same reagents is very important. Notwithstanding a similar reaction either during solvent casting and extrusion, the EVOH-SBO extrudates exhibit very different thermal and mechanical behavior from the solvent cast blends.[3] The most remarkable difference is that, while the new copolymer I has been shown amorphous in the case of the solvent cast blends,[3] the extruded I seems to be more crystalline than the starting neat EVOH copolymer. This structural difference appears also correlated to different mechanical behavior. Indeed, while the EVOH-FORSUD solvent cast film containing 6% FORSUD has been reported to exhibit higher Young modulus than the neat EVOH copolymer solvent cast film,[3] the extruded blend with the same composition has been shown in the present work to have nearly the same bending modulus (Table III) than the neat EVOH copolymer extrudate. Several factors may cause the above differences between the solvent cast and the extruded blends. These may be the higher processing temperature and higher applied shear rate of the extruded blend, the different forms of articles obtained, that is, films versus rods, and the presence of residual DMSO solvent in the solvent cast films. While the higher processing temperature and higher applied shear rate of the extrudates may be responsible of the higher crystallinity, for the solvent cast films the presence of residual DMSO, acting as compatibilizer, may modify the blend morphology-property connections. The above observed differences between solvent cast and extruded EVOH-SBO composite offer scope for further investigation. Two important facts are assessed in the present work. It is possible to process the EVOH-SBO also by extrusion, this technique being particularly suitable for use on an industrial scale. In addition, by reducing the amount of added SBO to 2 to 10% in the blend mix, no significant or great deterioration of the mechanical properties occurs relatively to those of the neat EVOH copolymer. The possibility to substitute part of the synthetic polymer with a waste derived biopolymer, while maintaining the same mechanical properties of the neat synthetic, is a step forward in the search of new biobased materials. This would allow reducing the exploitation of chemicals from fossil sources and of dedicated crops as source of biobased materials, and at the same time improving biowaste management practices through the valorization of biowaste as source of added value products. For the attainment of these perspectives, the data reported in the present work propose wide research potential for obtaining the EVOH-SBO in a variety of physical forms, such as extruded

sheets and blown films. The possible effect of DMSO determining the different mechanical properties of the solvent cast films suggests that a variety of formulations should be tested for the EVOH-SBO blends including additives to improve the compatibility of the synthetic copolymer and the biopolymer, and thus to optimize their performance in the intended application. The possibility to process the EVOH-SBO composites with different technologies and with different formulations offers several alternatives for further product development.

CONCLUSION

Amorphous lignin-like SBO obtained from fermented municipal biowastes mixed with poly vinyl alcohol-*co*-ethylene (38%) can be processed by solvent casting and melt extrusion to yield new materials. In both cases, evidence is provided for a condensation reaction, which occurs between EVOH and SBO and yields products where the biopolymer is covalently bonded to the synthetic polymer. These products have higher molecular weights and different thermal, rheological, and mechanical behaviors compared with the starting synthetic polymer. The properties of the blended materials depend on the type of fabrication process, and the chemical nature and relative content of the biopolymers. The data indicate potential for new worthwhile research aiming to the development of new materials, which contain biopolymers isolated from different wastes, in different physical forms, through different manufacture technologies, and using different formulations.

ACKNOWLEDGMENTS

REFERENCES

1. Babu, R. P.; O'Connor, K.; Seeram, R. *Progr. Biomater.* **2013**, *2*, 8.

2. Dorigato, A.; Pegoretti, A. *Colloid Polym. Sci.* **2012**, *290*, 359.

3. Franzoso, F.; Tabasso, S.; Antonioli, D.; Montoneri, E.; Persico, P.; Laus, M.; Mendichi, R.; Negre, M. *J. Appl. Polym. Sci.* **2015**, *132*, 1301.

4. Franzoso, F.; Causone, D.; Tabasso, S.; Antonioli, D.; Montoneri, E.; Persico, P.; Laus, M.; Mendichi, R.; Negre, M. *J. Appl. Polym. Sci.* **2015**, *132*, 5803.

5. Franzoso, F.; Antonioli, D.; Montoneri, E.; Persico, P.; Tabasso, S.; Laus, N. M.; Mendichi, R.; Negre, M.; Vaca-Garcia, C. *J. Appl. Polym. Sci.* **2015**, *132*, 6006.

6. Particle Sciences, Technical Brief, Volume *3*, **2010**. Available at: http://www.particlesciences.com/news/technical-briefs/2010/dissolving-films.html.

7. Siemann, U. *Progr. Colloid. Polym. Sci.* **2005**, *130*, 1.

8. Rosso, D.; Fan, J.; Montoneri, E.; Negre, M.; Clark, J.; Mainero, D. *Green Chem.* **2015**, *17*, 3424.

9. Chabrat, E.; Rouilly, A.; Evon, P.; Longieras, A.; Rigal, L. In Proceedings of the 24th Annual Meeting in Polymer Processing Society; Banff: Canada, **2010**. Available at: http://oatao.univ-toulouse.fr/. Eprints ID: 10596, p 1.

10. Yousfi, M.; Alix, S.; Lebeau, M.; Soulestin, J.; Lacrampe, M. F.; Krawczak, P. *Polym. Test.* **2014**, *40*, 207.

11. Nogueira, B. R.; Chinellato, A.; Ortiz, A. V.; Parveen, A.; Rangari, V. K.; Moura, E. A. B. In Handbook of Characterization of Minerals, Metals, and Materials; Hwang, J.-Y.; Monteiro, S. N.; Bai, C.-G.; Carpenter, J.; Cai, M.; Firrao, D.; Kim, B.-G., Eds.; Wiley: Hoboken, NJ, **2012**; Chapter 44, p 373.

12. Guirguis, O. W.; Moselhey, M. T. H. *Nat. Sci.* **2012**, *4*, 57.

13. Segal, L.; Creely, J. J.; Martin, A. E.; Conrad, C. M. *Text. Res. J.* **1959**, *29*, 786.

14. Silverstein, R. M.; Bassler, G. C. Spectrometric Identification of Organic Compounds, 2nd ed.; Wiley: New York, **1968**.

15. Ló pez-Rubio, A.; Lagaron, J. M.; Giménez, E.; Cava, D.; Hernandez-Muñoz, P.; Yamamoto, T.; Gavara, R. *Macromolecules* **2003**, *36*, 9437.

16. Gamon, G.; Evon, P.; Rigal, L. *Ind. Crops Prod.* **2013**, *46*, 173.

17. Ariff, Z. M.; Ariffin, A.; Jikan, S. S.; Rahim, N. A. A. In Rheological Behaviour of Polypropylene Through Extrusion and Capillary Rheometry, Polypropylene; Dogan, F. Ed.; Available at: http://www.intechopen.com/books/polypropylene/rheological-behaviour-of-polypropylene-through-extrusionand-capillary-rheometry.

18. Franco-Urquiza, E.; Santana, O. O.; Gámez-Pérez, J.; Martínez, A. B.; Maspoch, M. L. *Polym. Lett.* **2010**, *4*, 153.

19. Kalaprasad, G.; Mathew, G.; Pavithran, C.; Thomas, S. *J. Appl. Polym. Sci.* **2003**, *89*, 432.

20. Othman, N.; Azahari, N. A.; Ismail, H. *Malaysian Polym. J.* **2011**, *6*, 147.

21. Mngomezulu, M. E. Phase Change Materials Based on Polyethylene, Paraffin Wax and Wood Flour; University of the Free State (Qwaqwa Campus): Phuthaditjhaba, South Africa, **2009**; Available at: http://etd.uovs.ac.za/ETD-db/theses/available/etd-07232013102946/unrestricted/MngomezuluME.pdf.

22. Cerrada, M. L.; Perez, E.; Perena, J. M.; Benavente, R. *Macromolecules* **1998**, *31*, 2559.

23. Artzi, A.; Narkis, M.; Siegmann, A. *Polym. Eng. Sci.* **2004**, *44*, 1019.